Available online at www.sciencedirect.com
ScienceDirect
Trans. Nonferrous Met. Soc. China 27(2017) 2357−2362
Transactions of Nonferrous Metals Society of China
www.tnmsc.cn

Properties of AA7075 aluminum alloy in aging and retrogression and reaging process

Gokhan OZER, Ahmet KARAASLAN

Department of Metallurgical and Materials Engineering, Faculty of Chemistry and Metallurgical Engineering, Yildiz Technical University, Davutpasa-Esenler, Istanbul, 34210, Turkey

Received 28 October 2016; accepted 5 May 2017

Abstract: A retrogression process was applied to AA7075 alloy at 180, 240 and 320 °C for 1, 30, 50, 70, 90 and 120 min. After the retrogression, aging treatment was reapplied with T6 conditions (120 °C, 24 h). The mechanical properties of aged samples were determined by V-Charpy and hardness tests and also, physical properties of samples were determined by electrical conductivity tests. Moreover, microstructural properties were characterized by light microscope and transmission electron microscope. The results show that the effects of the temperature and the duration of the retrogression and reagent on the impact toughness and hardness are related to the precipitates at the grain boundary.

Key words: aluminum alloy; precipitate behavior; retrogression and reaging; impact toughness; hardness; electrical conductivity

1 Introduction

Aluminum and its alloys are the most important and frequently used materials in the world today due to their low density, high strength, easy processing, corrosion resistance and similar superior properties. Among the aluminum alloys, 7xxx series alloys form the preferred material group in aircraft and space industries and in military sector due to its high strength [1−5].

Precipitation hardening process applied to 7xxx series alloys is an important subject in metallurgy. Precipitation systems of 7xxx series alloy have been analyzed in many studies and precipitation sequence is usually accepted in the following way [6−15]:

Supersaturated solid solution→GP zones→metastable phase (η')→equilibrium phase (η).

Even though AA7075 alloy in T6 temper has the highest strength, at the same time it is particularly sensitive to stress corrosion cracking (SCC) and exfoliation corrosion. However, T73 heat treatment is used to increase corrosion resistance but decrease the strength of the alloy by 10%−15% [16,17]. In order to obtain mechanical strength and corrosion resistance, CINA and GAN [18] developed a specific heat treatment type named as retrogression and reaging (RRA).

This process is a multi-step heat treatment and is applied to the material in the T6 condition. Firstly, the material in T6 state is kept under heat treatment between 180−280 °C for a short period (5−2400 s). After that, the material is aged again in T6 conditions in the same way (120 °C, 24 h). After all the treatments, the material is cooled in water. Upon completing RRA treatment the material gains both corrosion resistance from the T73 condition and strength from the T6 condition [19]. The reason for that is stability of different phases and microstructure formation formed in RRA treatment. The microstructure changes that occur during RRA improve the properties of alloy in 7075-T6 condition:

These microstructure changes are:

1) The dissolving of GP zones;

2) Forming of tiny η' particles and their growth;

3) Primary coarsening of η particles followed by coarsening of grain boundary precipitate.

GP zones are formed by clustering dissolved Zn, Mg and Cu in a completely coherent with matrix. Semi-coherent η' phase is formed in grains in separate sheets. Stable equilibrium η phase, since it is an incoherent phase, settles at grain boundaries.

As a result, after the RRA condition in the structure of AA7075, there are very thin and homogeneously

Corresponding author: Gokhan OZER; E-mail:ozergokhan@gmail.com
DOI: 10.1016/S1003-6326(17)60261-9

distributed η' particles in the grains (similar to T6 condition) together with η ($MgZn_2$) precipitate at the grain boundaries distributed in the T73 condition. A microstructure like that shows why the AA7075 alloy after RRA treatment gains both corrosion resistance and mechanical strength [20].

It is well known that microstructure changes have important impacts on mechanical properties of alloys. It is important to understand the connection between the thermomechanical processes conducted and the mechanical properties obtained in order to develop high performance industrial alloys (yield strength, toughness, hardness). Despite many research conducted on this subject, the relation between tensile strength and hardness changes with impact toughness which has not yet been fully explained [21].

In this study, T651 samples were treated in RRA condition according to set conditions. Microstructure analysis, electrical conductivity, hardness and notch impact tests on different temperatures were conducted under the RRA condition. The focus point of the study is to establish causation in change of impact toughness, something not quite explained yet in the present literature.

2 Experimental

In this study, certified T651 applied AA7075 aluminum alloy in 10 mm-thick sheets was used. The chemical composition of the alloy is shown in Table 1.

Table 1 Chemical composition of AA7075 (mass fraction, %)

Si	Fe	Cu	Mn	Mg
0.1	0.19	1.53	0.07	2.55
Cr	Ni	Zn	Ti	Al
0.18	0.0058	5.89	0.024	Rest

Because alloy was in the T651 condition, the heat treatment was started directly from retrogression stage. RRA heat treatment was conducted owing to conditions determined in Table 2.

Table 2 RRA conditions of T651 sample

Retrogression			Re-aging	
Temperature/°C	Time/min	Cooling time/s	Temperature/°C	Time/h
180, 240, 320	1, 30, 50, 70, 90, 120	1−3	120	24

Hardness measurement was conducted using Brinell hardness (HB) measurement method. Hardness was characterized by HB type using 614 N of load and 2.5 mm ball in diameter.

Notch impact tests were conducted according to BS EN ISO 9016: 2012 standard in Mohr-Federhaff notch impact device with 300 J capacities.

Electrical conductivity measurements were applied by portable conductivity measurement device working according to GE Inspection 40I001 type Eddy current principle. Also, results were given in percentage due to International Annealed Copper Standard (IACS).

Metallographic sample preparation was carried out in accordance with standard sample preparing procedure. Moreover, samples were etched with Keller's reagent (95 mL pure water, 2.5 mL HNO_3, 1 mL HF and 1.5 mL HCl) for 1−4 min. Microstructural characterization was performed by using NIKON Eclipse MA100 optical microscope and NIS Elements BR Image Analysis software.

For transmission electron microscopy (TEM) studies, specimens were cut, and 3 mm-diameter discs were punched and ground to a thickness of less than 150 μm. Next, the specimens were perforated electro-polishing with an electrolyte solution of 25% nitric acit + 75% methanol at about 30 °C with 15 V in Struers-Tenupol-5 Double Jet Electropolisher. The foils were examined with a JEOL JEM 2100 HRTEM with a LaB6 filament, which was operated at 200 kV.

3 Results and discussion

3.1 Hardness

The hardness curves in the RRA conditions conducted with different heat temperatures and time periods are shown in Fig. 1.

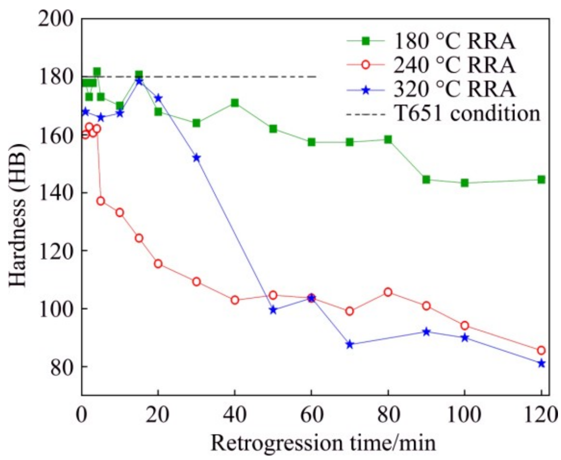

Fig. 1 Variation of hardness with retrogression time

As it can be observed from Fig. 1, when the retrogression temperature and duration time increase, hardness constantly decreases. Hardness decline slope decreases with increasing duration.

The first decline in hardness is related to the beginning of dissolving of fully coherent (GP zones) and semi coherent η' phase. Also, at the beginning of retrogression (until first 10 min), a re-increase of hardness can be observed. The reason for that is the forming of new nucleated η' phase over dissolved GP zones. The increase in volume ratio of this phase, as it is much more pronounced than in the T651 condition, provides greater hardness than that in T651 condition. With the increasing duration of the retrogression process, η' phase transforms into stable equilibrium phase, η phase.

This incoherent phase causes the hardness to decrease again [22−27]. This situation with hardness can also be explained as related to the overaging.

3.2 Electrical conductivity

Electrical conductivity changes of the material according to the RRA condition conducted with different heat temperatures and time are shown in Fig. 2.

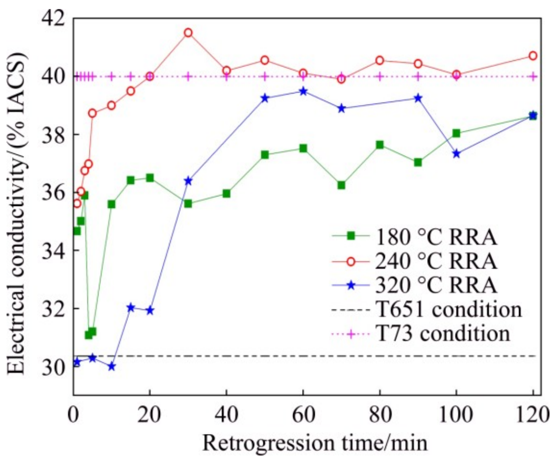

Fig. 2 Variation of electrical conductivity with retrogression time

When the retrogression period increases the electrical conductivity increases as well (Fig. 2). It can be observed from Fig. 2 that the results obtained from all retrogression periods and temperatures are higher than those from T651 condition.

As the period increases the precipitate starts to coarse and the distance between its particles starts to increase. As a result, the electron flow becomes easier and the electrical conductivity increases.

In the T651 condition, the coherent GP zones and the semi coherent η' phase enhance the lattice strain. This situation obstructs the electron flow. When the period and/or the temperature of retrogression increases, GP zones and η' phases dissolve. An incoherent η phase formed in their place decreases lattice distortion which facilitates electron flow, thus increasing the conductivity.

It has been pointed out in previous studies that there is a nonlinear connection between electrical conductivity and hardness [28,29]. In this study, inversely proportional relation between hardness and conductivity has been established (Fig. 3).

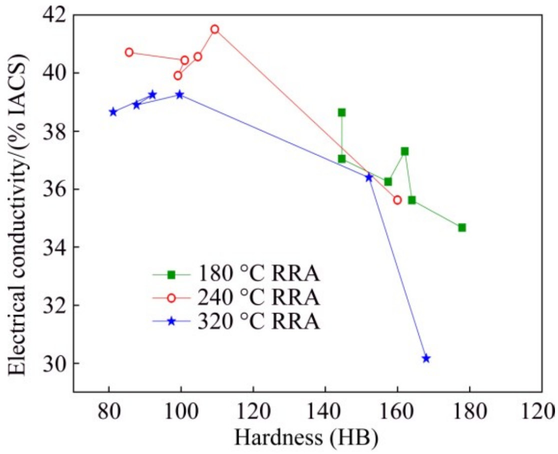

Fig. 3 Correlation between electrical conductivity and hardness

As it can be observed from Fig. 3, the relation between hardness and electrical conductivity is inversely proportional. As the retrogression temperature and time increase, the hardness decreases, while the conductivity increases.

3.3 Impact toughness

Impact toughness changes according to the RRA condition applied with different heat temperatures and time are shown in Fig. 4.

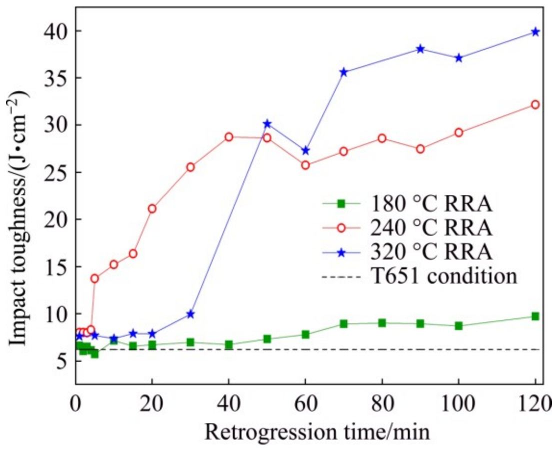

Fig. 4 Variation of impact toughness with retrogression time

When RRA heat temperatures are relatively low (180 °C) the impact toughness is similar to T651 impact toughness level. When the time at low RRA heat temperatures is increased, there is no significant change in impact toughness. For example, when being heated at 180 °C for 20 min under RRA condition, the impact toughness is 6.7 J/cm^2, while at 180 °C for 120 min in RRA condition, this value increases only to 9.7 J/cm^2. Despite that, when RRA heat temperatures rise, there is a dramatic change in impact toughness related to the time spent. When being heated at 320 °C for 20 min in RRA condition, the impact toughness is 7.84 J/cm^2, while at 320 °C for 120 min in RRA condition, this value increases to 39.9 J/cm^2 (Fig. 4)

At 180 °C, the change in impact strength for RRA treatments at different time is less than that for 240 °C and 320 °C RRA treatments. The impact strength at 240 °C for up to 50 min was higher than that at 320 °C.

The reason is that the RRA heat treatment at 240 °C for 50 min is to dissolve GP zones on one hand and to homogenously distribute the η' and η phases within the grain; on the other hand, the continuous network phase at the grain boundaries dissolves and becomes discontinuous. In the RRA processes performed at 320 °C for 50 min, although the continuous grain phase was found to be dissolved at the grain boundary, the coarsening of the precipitates in the grain caused the lowering of the strength. On the contrary, the continuous network phase at grain boundary with the RRA treatment at 320 °C for 50−120 min was more efficient than that treated at 240 °C, for 50−120 min and the spacing between them increased more. As a result, the impact strength values of all RRA processes performed at 320 °C for 50−120 min were above the impact values at 240 °C (Fig. 4).

The relation between impact toughness and hardness after RRA conditions at different temperatures and durations is given in Fig. 5. As it can be observed from Fig. 5, it is determined that when the impact toughness rises, the hardness decreases.

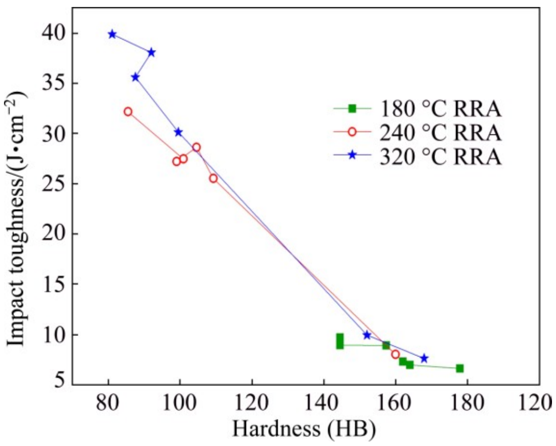

Fig. 5 Correlation between impact toughness and hardness

The increase in toughness along with the increase in duration time is related to the forming of precipitate in the microstructure and its distribution. In relation to the heat temperature and time, per unit volume distribution of the new η' phase formed in the dissolved GP zones is denser and also thinner. In this situation the hardness is higher than that obtained in the T651 condition. Naturally, in a result like this, the impact toughness is also higher. However, with the increase in time this semi coherent η' phase transforms into stable equilibrium phase, η phase, and this phase, being incoherent, causes the decrease in hardness. While the hardness decreases with the increase in retrogression time, the impact strength shows tendency to increase despite the forming of incoherent η phase. The reasons for that are as follows.

1) The increase in impact toughness together with the increase in retrogression time occurs because at the end of the RRA condition continuous and proportionally smaller stable equilibrium precipitate at the grain boundaries (η) coarsens and becomes discontinuous (unconnected to one another). In this way, previously blocked grain boundary line transformed by the forming of coarse and discontinuous η phase.

2) Because the continuous net structure is removed, the energy values of the area have changed as well. Also, the notch effect created at the grain boundary by the hard and brittle continuous net phase is decreased. The precipitate found in the continuous net form at the grain boundaries in T651 condition (Figs. 6(a) and 7(a)) provides hardness increase in these high energy areas, but as the precipitate is continuous it creates high notch effect. This also decreases the impact toughness of the material. However, with the increase of time and heat temperature after T651, the continuous net phase at the grain boundary is broken as it is explained above (Figs. 6(b) and 7(b)).

3) The breaking of the continuous net phase causes the precipitate to coarse and becomes spherical with the increase of heat temperature and time (Fig. 6(b)).

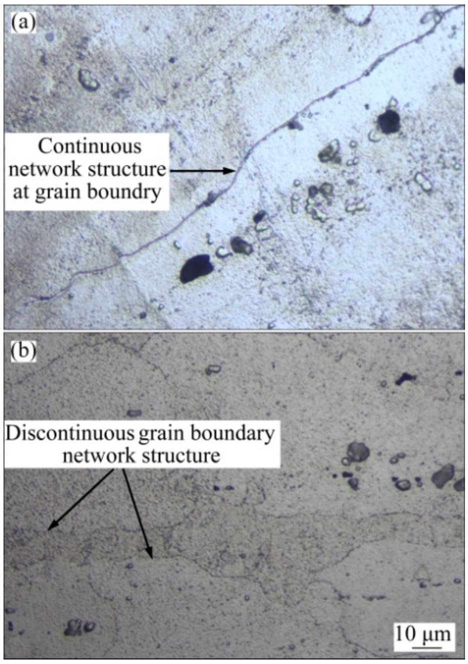

Fig. 6 Microstructures of AA7075 alloy treated in T651 condition (a) and in 240 °C for 90 min RRA conditions (b)

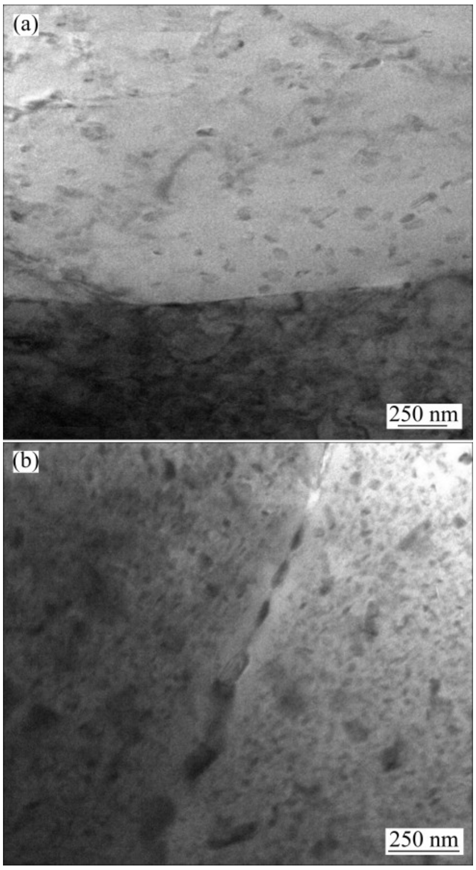

Fig. 7 TEM bright field images of AA7075 alloy treated in T651 condition (a) and in 240 °C for 90 min RRA conditions (b)

4) In this way, while the removal of the continuous net phase from the high energy grain boundaries increases free energy, the spherical precipitate decreases the notch effect in the structure.

In relation to the reasons explained above, with the increase in heat temperature and/or time the hardness decreases, while the strength increases.

4 Conclusions

1) When RRA heat treatment is conducted in relatively low temperatures (180 °C) and in short retrogression periods, the hardness is higher, compared with the T651 hardness value (HV 180), but with the increase of retrogression period it constantly decreases. The hardness constantly decreases at higher temperatures with increasing retrogression period. The highest hardness was obtained under RRA treatment at 180 °C for 4 min. The phases that provide the highest strength to the AA7075 alloy is coherent and semi coherent components. It is determined that when these phases dissolve, the hardness decreases.

2) The connection between the retrogression temperature and duration with the increase of electrical conductivity was determined. All the samples treated with RRA had higher electrical conductivity values compared with their starting state (T651). The highest conductivity value was observed heated at 240 °C RRA for 30 min. The coarsening of the precipitate caused by the prolonged time at the heat temperatures facilitates the electron flow in the matrix which increases the electrical conductivity. Also, the dissolution of the GP zones and semi coherent η' phase, which cause the electron flow to become difficult by causing the lattice strain, and formation of the dissolve and incoherent η phase is formed, thus incoherent η phase, reduces the lattice distortion and facilitates the electron flow, thus increases the conductivity.

3) When retrogression is conducted on relatively low temperatures (180 °C) the impact toughness is close to the T651 condition. When the temperature and time of RRA treatment are increased, the impact toughness increases as well. It is determined that when the increase in impact toughness is observed, the hardness decreases. The highest impact toughness was obtained at 320 °C RRA for 120 min, while the lowest hardness value is found in the same situation.

4) In relation to the temperature and duration of the RRA, the relation between impact toughness and hardness is explained by the morphology of the precipitate at the grain boundary. According to that, the increase in temperature and duration of the RRA treatments broke the continuous net phase structure and the notch effect in the structure diminished. As a result, the impact strength increased and the hardness decreased.

Acknowledgement

This project was supported by Yildiz Technical University Scientific Research Project Unit under Contract No: 2016-07-02-DOP02. The authors are grateful to Yildiz Technical University Scientific Research Project Unit for their financial supports.

References

[1] SU R M, QU Y D, LI R D, YOU J H. Influence of RRA treatment on the microstructure and stress corrosion cracking behavior of the spray-formed 7075 alloy [J]. Materials Science, 2015, 51: 372−380.

[2] SRINIVASAMURTHY P L, SARADA B N, KARTHIK B S, HOLLA S S. Effect of retrogression and reaging heat treatment on microstructure and corrosion properties of Al-7075 [J]. International Journal of Innovative Research in Science, Engineering and Technology, 2013, 2: 6434−6441.

[3] HOLT R T, RAIZENNE M D, WALLACE W, DuQUESNAY D L. RRA heat treatment of large Al 7075-T6 components [C]//New Metallic Materials for the Structure of Aging Aircraft. Corfu. Greece, 1999: 1−11.

[4] GOSWAMI R, LYNCH S, HOLROYD N J H, KNIGHT S P, HOLTZ R L. Evolution of grain boundary precipitates in Al 7075 upon aging and correlation with stress corrosion cracking behavior [J].

Metallurgical and Materials Transactions A, 2013, 44: 1268−1278.
[5] ZAID H R, HATAB A M, IBRAHIM A M A. Properties enhancement of Al−Zn−Mg alloy by retrogression and re-aging heat treatment [J]. Journal of Mining and Metallurgy Section B: Metallurgy, 2011, 47(1) B: 31−35.
[6] LIN Y C, ZHANG Jin-long, LIU Guan, LIANG Ying-jie. Effects of pre-treatments on aging precipitates and corrosion resistance of a creep-aged Al−Zn−Mg−Cu alloy [J]. Materials & Design, 2015, 83: 866−875.
[7] STARINK M J, WANG S C. A model for the yield strength of overaged Al−Zn−Mg−Cu alloys [J]. Acta Materialia, 2003, 51: 5131−5150.
[8] BARTGES C W. Changes in solid solution composition as a function of artificial ageing time for aluminium alloy 7075 [J]. Journal of Materials Science Letters, 1994, 13: 776−778.
[9] PENG Guo-sheng, CHEN Kang-hua, CHEN Song-yi, FANG Hua-chan. Influence of dual retrogression and re-aging condition on microstructure strength and exfoliation corrosion behavior of AlZnMgCu alloy [J]. Transactions of Nonferrous Metals Society of China, 2012, 22: 803−809.
[10] SHA G, CEREZO A. Early-stage precipitation in Al−Zn−Mg−Cu alloy (7050) [J]. Acta Materialia, 2004, 52: 4503−4516.
[11] ESMAILIAN M, SHAKOURI M, MOTTAHEDI A, SHABESTARI S G. Effect of T6 and re-aging heat treatment on mechanical properties of 7055 aluminum alloy [J]. International Journal of Chemical, Molecular, Nuclear, Materials and Metallurgical Engineering, 2015, 9−11: 1230−1233.
[12] XU Xiao-feng, ZHAO Yu-guang, MA Bing-dong, ZHANG Ming. Electropulsing induced evolution of grain-boundary precipitates without loss of strength in the 7075 Al alloy [J]. Materials Characterization, 2015, 105: 90−94.
[13] DESCHAMPS A, BRECHET Y. Influence of quench and heating rates on the ageing response of an Al−Zn−Mg−(Zr) alloy [J]. Materials Science and Engineering A, 1998, 251: 200−207.
[14] MA Ka-ka, WEN Hai-ming, HU Tao, TOPPING T D, ISHEIM D, SEIDMAN D N, LAVERNIA E J, SCHOENUNG J M. Mechanical behavior and strengthening mechanisms in ultrafine grain precipitation- strengthened aluminum alloy [J]. Acta Materialia, 2014, 62: 141−155.
[15] STARINK M J, LI X M. A Model for the electrical conductivity of peak-aged and overaged Al−Zn−Mg−Cu alloys [J]. Metallurgical and Materials Transactions A, 2003, 34: 899−911.
[16] FOOLADFAR H, HASHEMI B, YOUNESI M. The effect of the surface treating and high-temperature aging on the strength and SCC susceptibility of 7075 aluminum alloy [J]. Journal of Materials Engineering and Performance, 2010, 19(6): 852−859.
[17] MARLAUD T, MALKI B, HENON C, DESCHAMPS A, BAROUX B. Relationship between alloy composition, microstructure and exfoliation corrosion in Al−Zn−Mg−Cu alloys [J]. Corrosion Science, 2011, 53: 3139−3149.
[18] CINA B M, GAN R. Reducing the susceptibility of alloys particularly aluminum alloys to stress corrosion cracking: US Patent, 3856584 [P]. 1974−12−24.
[19] REDA Y, ABDEL-KARIM R, ELMAHALLAWI I. Improvements in mechanical and stress corrosion cracking properties in Al-alloy 7075 via retrogression and re-aging [J]. Materials Science and Engineering A, 2008, 485: 468−475.
[20] OLIVEIRA A F Jr, de BARROS M C, CARDOSO K R, TRAVESSA D N. The effect of RRA on the strength and SCC resistance on AA7050 and AA7150 aluminium alloys [J]. Materials Science and Engineering A, 2004, 379: 321−326.
[21] CHEMINGUI M, KHITOUNI M, JOZWIAK K, MESMACGUE G, KOLSI A. Characterization of the mechanical properties changes in an Al–Zn–Mg alloy after a two-step ageing treatment at 70 °C and 135 °C [J]. Materials and Design, 2010, 31: 3134−3139.
[22] MARLAUD T, DESCHAMPS A, BLEY F, LEFEBVRE W, BAROUX B. Evolution of precipitate microstructures during the retrogression and re-ageing heat treatment of an Al−Zn−Mg−Cu alloy [J]. Acta Materialia, 2010, 58: 4814−4826.
[23] DANH N C, RAJAN K, WALLACE W. A TEM study of microstructural changes during retrogression and reaging in 7075 aluminum [J]. Metallurgical Transactions A, 1983, 14: 1843−1850.
[24] PARK J K, ARDELL A J. Effect of retrogression and reaging treatments on the microstructure of Al-7075-T651 [J]. Metallurgical Transactions A, 1984, 15−18: 1531−1543.
[25] LACOM W. Calorimetric investigations strengthened 7075 in a dispersion alloy [J]. Thermochimica Acta, 1996, 271: 93−100.
[26] ADLER P N, DeIASI R. Calorimetric studies of 7000 series aluminum alloys: II. Comparison of 7075, 7050, and RX720 alloys [J]. Metallurgical Transactions A, 1977, 8: 1185−1190.
[27] FANDREATTA F, TERRYN H, de WIT J H W. Effect of solution heat treatment on galvanic coupling between intermetallics and matrix in AA7075-T6 [J]. Corrosion Science, 2003, 45: 1733−1740.
[28] GÜR C H, YILDIZ I. Non-destructive investigation on the effect of precipitation hardening on impact toughness of 7020 Al−Zn−Mg alloy [J]. Materials Science and Engineering A, 2004, 382: 395−400.
[29] SALAZAR-GUAPURICHE M A, ZHAO Y Y, PITMAN A, GREENE A. Correlation of strength with hardness and electrical conductivity for aluminium alloy 7010 [J]. Materials Science Forum, 2006, 519−521: 853−858.

回归再时效处理过程中 AA7075 铝合金的性能

Gokhan OZER, Ahmet KARAASLAN

Department of Metallurgical and Materials Engineering, Faculty of Chemistry and Metallurgical Engineering, Yildiz Technical University, Davutpasa-Esenler, Istanbul, 34210, Turkey

摘　要：采用回归法分别在 180、240 和 320 °C 下热处理 AA7075 铝合金 1、30、50、70、90 和 120 min。回归处理后，再在 T6(120 °C，24 h)热处理制度下对合金进行时效处理。通过 V 型冲击和硬度测试确定时效样品的力学性能，并通过测定电导率确定样品的物理性能。此外，利用光学显微镜和透射电镜表征合金的显微组织性能。结果表明，回归再时效的温度和时间对合金冲击韧性和硬度的影响与晶界的析出相有关。

关键词：铝合金；析出行为；回归再时效；冲击韧性；硬度；电导率

(Edited by Xiang-qun LI)